International Journal of Nanomaterials and Chemistry

http://dx.doi.org/10.12785/ijnc/010302

One-Step Functionalization of Silver Nanoparticles Using the Orsellinic Acid Compound Isolated From the Endophytic Fungus *Epicoccum Nigrum*: Characterization and Antifungal Activity

Mohamed A. Mohamed [1,2,*].

[1]Instituto de Biología Molecular y Celular de Plantas (Consejo Superior de Investigaciones Científicas - Universidad Politécnica de Valencia), Avenida de los Naranjos, 46022 Valencia, Spain.
[2]Plant Pathology Research Institute, Agricultural Research Center, Giza 12655, Egypt.

Received: 14 May 2015, Revised: 16 Jun. 2015, Accepted: 18 Jun. 2015.
Published online: 1 Sep. 2015.

Abstract: A simple green method for the synthesis of silver nanoparticles (AgNPs) using the natural isolated orsellinic acid compound has been investigated for the first time. The present work describes a one-step functionalization of AgNPs using orsellinic acid as a reducing agent to convert Ag+ cations to AgNPs. This process eliminates the use of external toxic chemical reducing agents to provide a completely green synthetic route. The biosynthesized AgNPs were characterized by means of high spectroscopic and microscopic techniques. The results showed the formation of high crystalline spherical AgNPs with an average diameter of 22.5 ±1.8 nm. Moreover, the Fourier transform infrared (FT-IR) analysis indicated that AgNPs are covered with a thin layer of biomoieties on their surface and suggested that the hydroxyl groups of orsellinic acid compound are involved in the reduction of the Ag+ ions, capping and stabilizing the formed nanoparticles. Remarkably, the formed AgNPs showed potent antifungal activity against the phytopathogenic fungus *Alternaria solani* causing early blight disease of tomato plants. Those findings emphasize that such biocompatible green silver nanoparticles with their excellent antifungal activities may find their applications as new bio-fungicides against various plant pathogenic fungi in the field of crop improvement and plant disease management.

Keywords: Silver nanoparticles, biosynthesis, orsellinic acid, *Epicoccum nigrum*, antifungal activity.

1 Introduction

Nanotechnology is a fast-developing cutting-edge technology with wide-ranging applications in different areas of science and technology [1-5]. One of the important aspects in the field of nanotechnology is the development of more reliable and safe processes for the synthesis of nanomaterials over a range of sizes and well chemical composition [6]. Among all the metal nanoparticles, silver nanoparticles (AgNPs) find its way in different fields particularly in medicine and agricultural nanotechnology due to their unique antimicrobial properties [7-8]. A multitude of chemical and physical methods have been established to synthesize silver nanoparticles, including conventional chemical reduction protocols utilizing citrate, ascorbate, sodium borohydride, and hydrazine as reducing agents[9-10], spray pyrolysis [11], physical vapor deposition [12] and irradiation route [13]. Since most processes described so far are associated with high energy consumption or involve toxic chemicals that are not considered environmentally benign. Hence, a renewed interest has been therefore generated on the adoption of safe, cost-effective, non-toxic and greener approaches for nanoparticle synthesis using microorganisms [14-18]. Fungi are considered the best option compared to other eukaryotes [19]. The huge interest of fungi as green nano-factories backed to the vast repertoire of proteins, enzymes, and other bioactive secondary metabolites they produce which possess redox capacity, thereby significantly making downstream processing quite easy and increasing the productivity of this biosynthesis approach [20]. Recently, fungal endophytes have been recognized as important sources of a variety of structurally novel active secondary metabolites with unique chemical, physical properties and other biological activities [21-23]. Furthermore, those biomolecules can easily undergo highly controlled, hierarchical assembly [24], which makes them suitable for the development of reliable and ecofriendly processes for metal nanoparticle synthesis [25]. However, up to date, very few studies have investigated the biological synthesis of AgNPs using natural compounds [26-27]. To the best of our knowledge, the use of biomolecules derived fungi has not been investigated so far for their ability in biosynthesis

* Corresponding author E-mail: mohammed_sharouny@yahoo.com

of nanoparticles, hence much attention has been directed toward synthesizing AgNPs using this new green route. Despite the antimicrobial potential of AgNPs, few reports are available on the use of AgNPs as safe alternatives to chemical fungicides in plant disease management especially against fungal pathogens [28-33].The objectives of the present study was to biosynthesize AgNPs using new green approach through biomolecules derived fungi, more specifically the orsellinic acid compound, and characterize the formed AgNPs utilizing UV-visible spectroscopy, High Resolution Transmission electron microscope (HR-TEM), Energy dispersive X-ray spectroscopy (EDX), X-ray diffraction (XRD), and Fourier transform infrared spectroscopy (FT-IR) analysis. Besides, evaluation their antifungal activity against *Alternaria solani* the causal agent of tomato early blight disease.

2 Material and Methods

2.1 Sample collection and isolation of endophytic fungi

Fresh healthy leaves of *Helianthemum hirtum* (L.) Miller were collected from the northern part of El Alameen (Egypt) in 2014. The samples were collected in sterile plastic bags and kept cool until transported to laboratory for further processing. The samples were washed under running tap water and air-dried. Surface sterilization was done by immersing the cleaned leaves in 70% ethanol three times for 2 minutes followed by rinsing in sterilized deionized water. The surface-sterilized leaves were cut into small pieces using a sterile blade and placed on Potato dextrose agar (PDA) plates containing 250 mgL^{-1} streptomycin for further incubation at 28 °C [34]. The hyphal tip of the endophytic fungi growing out from the plant tissues was cut with a sterile Pasteur pipette and transferred onto new PDA plates for purification and finally incubated at 28 ◦C for 8 days for identification.

2.2 Identification of the endophytic fungus Epicoccum nigrum

After incubation period, the endophytic fungus *Epicoccum nigrum* was firstly identified based on its morphological and microscopic characteristics recorded in different mycological keys [35-36]. Consecutively, the identification was confirmed at molecular level using PCR amplification of the ribosomal internal transcribed spacer (ITS) region with universal primers ITS1 and ITS4. For the ITS based sequencing, the genomic DNA was extracted from 100 mg mycelium. The mycelium was scrapped off and washed well in sterile nano-pure water. DNA extraction was done by DNEasy Plant Mini Kit (Quigen USA). The primers used were ITS1 (5'-CTTGGTCATTTAGAGGAAGTAA-3') and ITS4 (5'-TCCTCCGCTTATTGATATGC-3') [37]. The amplification protocol used was GeneAmp 9700, max ramp rate: (ITS1-ITS4). The amplified DNA was purified and directly sequenced using the same primers. BLASTN 2.2.18+ was used to search for similar sequences in GenBank.

2.3 Extraction and purification of Epicoccum nigrum metabolites

For small scale metabolites extraction, six active grown agar plugs from the isolated fungal culture were sonicated for 30 min with 1 mL ethyl acetate:dichloromethane:methanol (3:2:1) buffered with 1% formic acid [38]. The extract were then lyophilized and dissolved ultrasonically in 500 µL methanol and initially analyzed on an Agilent 1260 LC system (Agilent Technologies, Waldbronn, Germany) equipped with a diode array detector. Five µL samples were injected and separated on a 100 x 2.1 mm kinetex 2.6 µm Hexyl-Phenyl (Phenomenex, Torrance, CA, USA) using a flow of 0.4 mL/min with a linear water-acetonitrile gradient. The gradient started at 10% acetonitrile and reached 100% acetonitrile in 20 min, which were held for 5 min. The extracts were subsequently analyzed and mass spectra were collected using ultrahigh-performance liquid chromatography combined with high resolution mass spectrometry (UHPLC-HRMS) on an Agilent 1290 UHPLC system (Agilent technologies, Santa Clara, CA, USA) equipped with a 25 cm, 2 mm ID, 2.6 µm Agilent Poroshell phenyl hexyl column, and coupled to an Agilent 6550 quadrupol. For large structure elucidation, fungal metabolites were extracted from 25 PDA plates of three weeks old cultures by subjected to ultrasonic treatment for 45 min in ethyl acetate buffered with 1% formic acid. The crude extract was then resuspended in 20 mL methanol after evaporation and then fractionated on a Strata Silica C18-E (55 µm, 70 Å), 50 g/150 mL, Giga Tube (Phenomenex, Torrance, CA, USA). The extract were loaded on the column in a 10% methanol solution, washed with 200 mL 20% methanol and eluted with the same amount with 40% acetonitrile. The final purification was performed by multiple cycles on an Agilent 1260 semi-preparative HPLC system (Phenomenex, Torrance, CA, USA). 40 µL crudely purified metabolites were injected on the HPLC column using a flow of 5 mL/min with a linear water-acetonitrile gradient. The gradient started at 0% acetonitrile and reached 60% acetonitrile in 10 min, which were held for 1 min before reverting to 0% acetonitrile.

Structural verification

Nuclear magnetic resonance spectroscopy (NMR) on a Bruker AVIII-600 spectrometer (Bruker, Karlsruhe, Germany) was used to verify the sturcture of the isolated compound. Approximately 5 µg of the isolated compound was dissolved in 600 µL CDCl3 and analyzed with ^{1}H and ^{13}C at 291K. Spectra were recorded and analyzed with Top Spin 3.2 (Bruker). Residual solvent signals were used as internal standards (reference signal). The observed

chemical shift (ϵ) values were given in ppm and the coupling constants (J) in Hz.

2.4 Extracellular synthesis of silver nanoparticles

The formation of silver nanoparticles using the orsellinic acid was firstly evaluated visually by observing the color change of $AgNO_3$ solution. In a typical synthesis of AgNPs, 5 mL (1 mg/10 mL) of orsellinic acid was added drop by drop to 20 ml of 1 mM $AgNO_3$ aqueous solution with stirring magnetically under ambient conditions. The reaction mixture was then incubated at 25°C in dark conditions (to avoid photochemical reduction) and was routinely monitored for visual colour change and further confirmed by UV–vis spectroscopy.

Characterization of silver nanoparticles

UV-Vis spectroscopic analysis

The bioreduction of Ag+ ions to Ag^0 by the orsellinic acid was monitored using Shimadzu UV-vis spectrophotometer operated at a resolution of 1 nm. A small aliquot (2 mL) of the colored suspended particles was taken in a quartz cuvette after changing in color mixture and observed for wavelength scanning ranging between 300-800 nm at different time intervals with distilled water as a reference.

Purification of AgNPs

The AgNPs solution was centrifuged at 14,000 rpm for 20 min. The supernatant was discarded and the nanomaterial pellets was dispersed with deionized water and centrifuged three times to remove the free entities and unbound biological molecules from the formed AgNPs. The purified pellets were dried in 60 °C for further characterization.

High Resolution Transmission Electron Microscopy (HR-TEM)

For HR-TEM measurements, a drop of AgNPs solution was placed on the carbon coated copper grid (carbon type-B, 300 mesh, Ted Pella, Inc., Redding, CA, USA), and kept for 3 hours under vacuum desiccation. The carbon coated copper grids were then loaded onto a specimen holder. The HR-TEM micrographs were taken using the JEOL JSM 100CX TEM (Jeol, Japan) operated at an accelerating suitable voltage (kV). The images were analyzed using Image J software and the average particle size was calculated. Additionally, selected area Electron Diffraction (SAED) of the nanoparticles was also analyzed using HR-TEM.

Energy Dispersive X-ray photometric analysis (EDX)

EDX analysis was performed by energy-dispersive spectroscopy (EDS) using INCA Energy TEM 200 with analysis software (JEOL) for identifying the elemental composition of the biosynthesized AgNPs and the purity.

X-ray diffraction analysis (XRD)

The X-ray diffraction techniques were used to determine the crystalline structure of the purified silver nanoparticles and also to roughly estimate the size of the nanocrystallites. A film of the biologically synthesized Ag-NPs were cast into glass slides and subjected to X-ray diffraction analysis carried out using Phillips PW 1830 instrument Powder. The operating voltage of 40 kV and current of 30 mA with Cu k_α radiation of 0.1541 nm wavelength, in the 2θ range 10-80º, step size 0.02/θ. The images obtained were compared with standards to account for the crystalline structure.

Fourier transform infrared spectroscopy (FT-IR)

Fourier transform infrared analysis was evaluated to determine the possible functional groups in orsellinic acid responsible for bio-reduction of Ag+ ions and formation of AgNPs. For sample preparation, 300 µl of concentrate colloidal silver nanoparticle solution was mixed with 10 mg potassium bromide (KBr) in clean crucible, until it becomes a fine powder. The sample was prepared and oven dried to remove the traces of moisture. The FT-IR spectrum was recorded using Jasco FT/ IR-6300 Fourier transform infrared spectrometer equipped with JASCO IRT-7000 Intron Infrared Microscope using transmittance mode operating at a resolution of 4 cm^{-1}(cm21) (JASCO, Tokyo, Japan) [39].

Assessment of antifungal activity *in Vitro*.

The antifungal activity of the biosynthesized AgNPs was evaluated by the agar dilution method on three different pathogenic isolates of *Alternaria solani*, the causal agent of tomato early blight disease. The agar medium was supplemented with three different concentrations of the AgNPs (5, 10, 20 ppm). A 1.5 diameter grown mycelial disc of *Alternaria solani*, was taken from the edge of active growth fungal culture, and placed in the center of each plate. Control plates were included without the addition of AgNPs. The inoculated plates were then incubated at 25◦C for 8 days. The percentage of fungal mycelial inhibition rate was recorded everyday up to 8 days and calculated according to the following equation:

$$\text{Inhibition rate (\%)} = R - r / R \times 100$$ [40]

"Where $\boldsymbol{R}$ is the radial growth of fungal hyphae on the control plate and $\boldsymbol{r}$ is the radial growth of fungal hyphae on the plate supplemented with AgNPs"**.** All experiments were conducted in triplicate under sterile conditions.

3 Results and Discussion

3.1 Identification of the endophytic fungus

A total of 15 endophytic fungal species were obtained from 65 healthy leaf segments tissues of *Helianthemum hirtum* (L.) Miller, representing a rate of colonization of 23.1 %. Of the 15 endophyte taxa obtained, 10 were identified to the species level, two to the genus level, while three did not form reproductive structures (sporophores and spores) and were termed morphotaxa 1, 2 and 3 (Table 1). The most

dominant species was *Curvularia lunata*, corresponding to (60%), followed by *Epicoccum nigrum* (43.3%) of the total fungal colonies obtained.The morphological microscopic examination of *Epicoccum nigrum* isolate showed that the

Table 1: Showing the composition of the isolated endophytic fungal taxa and frequency of colonization (%).

Endophytic fungi	No. of records	Frequency (%)
***Curvularia lunata* Boedijn (Mitrai)**	**90**	**60**
***Epicoccum nigrum* (Link)**	**65**	**43.3**
***Cladosporium oxysporum* (Berk. & M.A. Curtis)**	**40**	**26.6**
***Cladosporium cladosporioides* (Fresen.) G. A. de vries**	**50**	**33.3**
***Aspergillus niger* (Tiegh.)**	**20**	**13.3**
***Aspergillus nidulans* (Eidam)**	**18**	**12**
***Aspergillus terrus* (Thom)**	**9**	**6**
***Chaetospermum* gossypinum Nag Raj (G. F. Atk.)**	**22**	**14.6**
***Savoryella lignicola* (E. B. G. Jones & R. A. Eaton)**	**7**	**4.66**
***Alternaria alternata* (Fr) Keissl**	**33**	**22**
***Chaetospermum gossypinum* Nag Raj (G. F. Atk.)**	**7**	**4.66**
***Drechslera hawaiiensis* (Bugnic. ex Subram. & B.L. Jain)**	**2**	**1.33**
Morphotaxon 1	**4**	**2.66**
Morphotaxon 2	**2**	**1.33**
Morphotaxon 3	**1**	**0.66**

colony with aerial mycelia interspersed with dark cushion-shaped sporodochia consists of short, compact conidiophores bearing globose, pyriform conidia with mostly 14-26 µm diameter with a funnel-shaped base. The identity of the fungal isolate was also confirmed based on analyses of the nucleotide sequence of the nuclear ribosomal ITS region. An analysis of DNA sequence similarity among sequences lodged in GenBank revealed that the ITS1-5.8S-ITS2 region of the isolated fungus showed 98.7% homology to that of *Epicoccum nigrum* OTU1070 (GU934519).

3.2 Orsellinic acid as an extracellular product of Epicoccum nigrum

After partitioning, the EtOAc extract of *Epicoccum nigrum* between n-hexane and 90% aqueous MeOH, the MeOH phase was fractionated by vacuum liquid chromatography (VLC) on silica gel, followed by size exclusion chromatography and semi preparative HPLC, to yield the fungal compounds. A well resolved peak eluting at 18 min, corresponding to the retention time of orsellinic acid was collected. Orsellinic acid was purified as yellowish needles (20 mg) and displayed UV absorbances at ƛmax (MeOH) 223.1, 261.3 and 298.5 nm. The Mass spectra (MS) showed molecular ion peaks at *m/z* 169.0 $[M+H]^+$ (base peak) and *m/z* 167.4 $[M-H]^-$ (base peak), respectively, indicating a molecular weight of 168 g/mol g/mol (Figure 1 a, b). ^1H and ^{13}C NMR spectra indicated the presence of an aromatic methyl group at δH 2.38 and αC 23.4 as well as a pair of *meta*-coupled protons at δH 6.16 and 6.11 (each d, *J*=2.2 Hz) assigned to H-3 and H-5, respectively (see Table 2). Additionally, the ^{13}C NMR spectrum contained 6 aromatic carbon signals, two of which were hydroxylated, and a signal at δC 173.2 indicative of an aromatic carboxylic acid

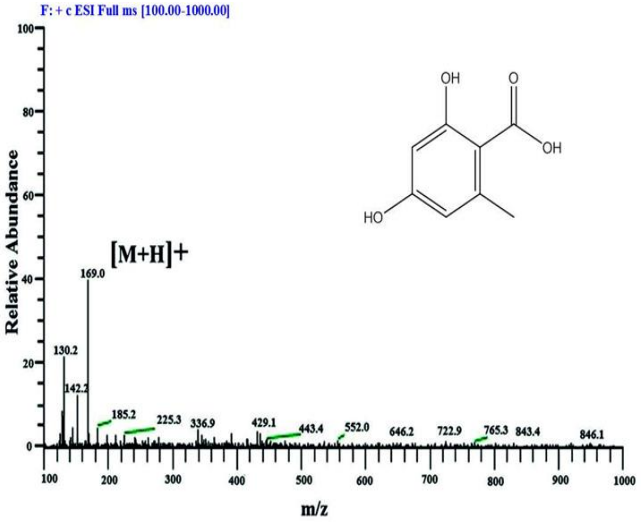

Fig.1 A

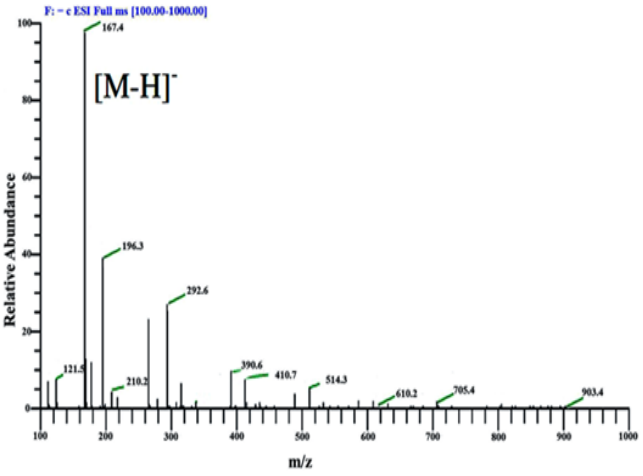

Fig.1 B

Fig.1 (A, B). Mass spectra of Orsellinic acid compound.

function (Table 2). The ^{13}C, ^1H NMR and mass spectra exhibited that the isolated compound has eight carbon atoms and supported a molecular formula of $C_8H_8O_4$. The obtained data were found to be almost identical to published ones for orsellinic acid [41]. Orsellinic acid was previously isolated from the fungus *Penicillium* sp. and lichens [42-43].

3.3 Biosynthesis of silver nanoparticles

The formation of silver nanoparticles using the orsellinic acid was firstly evaluated visually by observing the color change of $AgNO_3$ solution after challenging with 5 ml of

the orsellinic acid. The results showed changing in the mixture color which began to turn into dark yellow after 30 minutes denoting the reduction of silver cations and formation of silver nanoparticles. The solution color intensified to be darker with time as shown in (Figure 2). Moreover, the UV–Vis spectroscopic analysis of AgNPs solution showed a strong absorbance peak centered at 440-450 nm at different time intervals which is characteristic for surface Plasmon resonance of silver and hence indicate the

Table 2: ^{1}H, ^{13}C NMR data of isolated compound at 500 (^{1}H) and 125 (^{13}C) MHz

Nr.	δ_H (DMSO-d_6)	δ_C (DMSO-d_6)	δ_H (MeOD)
1		104.8	
2		161.9	
3	6.11, d (2.2 Hz)	100.4	6.20, br s
4		164.4	
5	6.16, d (2.2 Hz)	110.9	6.20, br s
6		142.8	
CH3	2.38, s	23.4	2.54, s
COOH		173.2	
2-OH	12.63, br s		
4-OH	10.13, br s		

formation of AgNPs (Figure 2). Furthermore, it was observed that with increase in time, there was an increase in absorbance which ultimately indicated the increase in concentration of AgNPs with time. indicating more reduction of Ag+ ions and formation of more AgNPs.

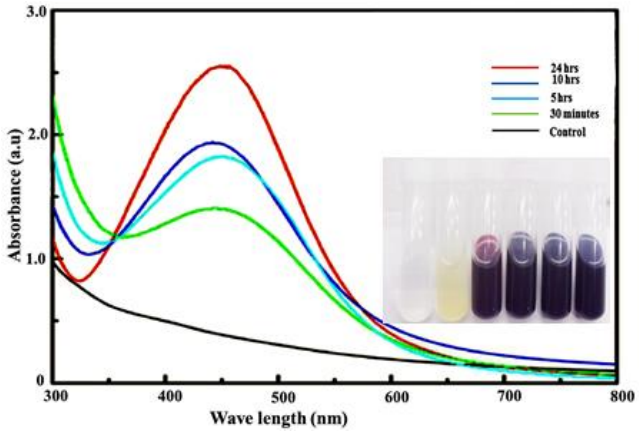

Fig.2: showing UV spectra of AgNPs at different time intervals.

Characterization studies

The HR-TEM measurements reveal the size, shape and morphology of the biologically synthesized AgNPs. The HR-TEM images, indicated the formation of spherical and poly-dispersed AgNPs with an average particle size of 22.5 ±1.8 nm (discrete 120 NPs) (Fig. 3 a, b,c). Moreover, the images clearly show the presence of a thin layer of the capping agent used (orsellinic acid) surround the formed particles (see Fig. 3a). The SAED pattern shows circular rings which can be indexed corresponding to the reflections from the (111), (200), (220) and (311) planes (JCPDS 04-0783). These planes correspond to fcc Ag and reveal the highly crystalline nature of the synthesized silver nanoparticles (Fig. 4).The crystalline nature of the formed AgNPs was also further confirmed by XRD analysis (Fig. 5). The XRD pattern revealed the typical fcc structure of Ag NPs [44].

The XRD spectra showed four main characteristic Bragg diffraction peaks at 2θ values of nearly 37°, 46°, 66°, and 77°.These diffraction peaks can be attributed to the (111), (200), (220), and (311) planes of silver respectively (JCPDS: File No. 4-783). This indicates the nanoparticles are face centre cubic and well crystalline in nature.The EDX spectrum showed a strong typical optical absorption peak at approximately 3 keV, which was attributed to the Surface plasmon resonance (SPR) of the metallic Ag nano crystals [45]. The EDX spectrum also shows other bands for Carbon and Oxygen peaks beside Ag peak (Figure 6), which appeared due to the scattering caused by the capping agent used which bound to silver surface. Furthermore, the FT-IR spectrum of the orsellinic acid indicated absorption peaks at 3386 (OH), 2935 (C-H), 1623 (C=O), 1408 (C=C), 1078 (C-O), 779, 604, and 1071cm^{-1}. Compared to that of the formed AgNPs, the absorption peaks were shifted to 3463, 1591, 1385, 1023 and 604 cm^{-1}.

Based on the mentioned IR results, the absence of aliphatic C-H stretching group and shift of both O-H and C=O groups to 3463 and 1591 cm^{-1} respectively, suggested that both hydroxyl and carbonyl groups are involved in reduction of Ag+ ions and indicating that those groups have stronger ability to bind metal and form silver nanoparticles. This also suggests that biomolecules derived fungi are an interesting rapid green route in biosynthesis of AgNPs, which can be possibly exploited by doing dual functions of reduction and stabilization of different nanomaterials (i.e silver nanoparticles) in biosynthesis process.

Antifungal activity of AgNPs

The antifungal activity of the biosynthesized AgNPs was performed with different concentrations (10, 20 and 50 ppm) against the phytopathogenic fungus *Alternaria solani* (Fig. 7a). The obtained results clearly revealed significant inhibition in the mycelial growth of *Alternaria solani*, to various extents with increasing concentration of AgNPs (Fig. 7 b). These results correlated well with previous reports strongly suggest that the biologically formed

AgNPs could be used as potent green antifungal alternatives to conventional chemical fungicides [46]. Through this juncture, it is of paramount important to understand the mode of action of silver nanoparticles as antimicrobials. Though it is not well understood till now, but some hypotheses arise to validate the antifungal activity of those nanomaterials [47-49]. Few studies suggested that the potent antimicrobial activity of AgNPs may be backed to the free radicles formation by those nanomaterials which could disturb the membrane lipids and then finally spoil the fungal membrane functions [50].

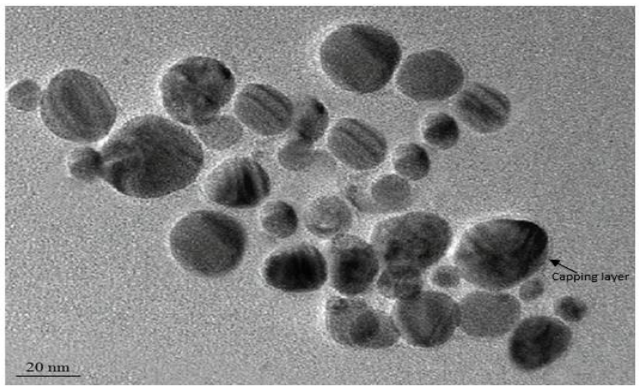

Fig. 3A

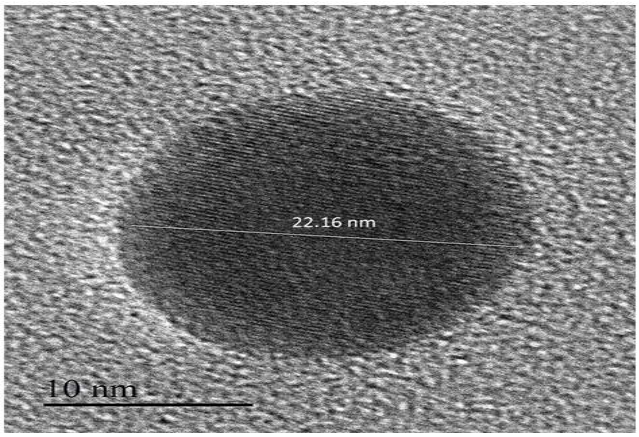

Fig. 3B

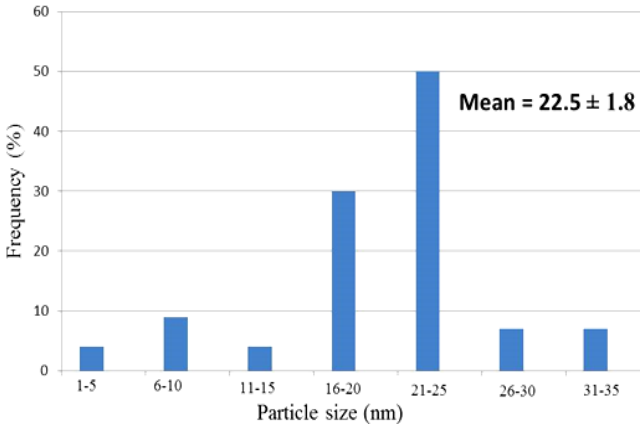

Fig. 3C

Fig. 3A, B. HR-TEM images of AgNPs synthesized by the reduction of Ag^{+} using orsenillic acid compound. **Fig. 3C:** Particle mean sizes (nm) as obtained by HR-TEM measurement for orsenillic acid mediated synthesis of silver nanoparticles.

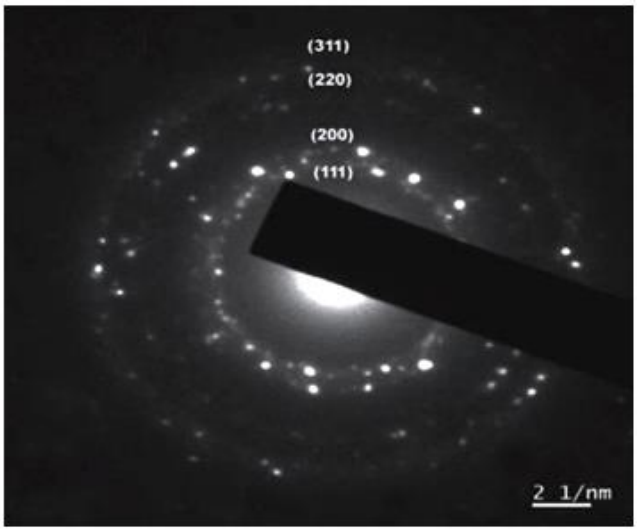

Fig. 4: Selected area of electron diffraction (SAED) pattern of randomly selected silver nanoparticles.

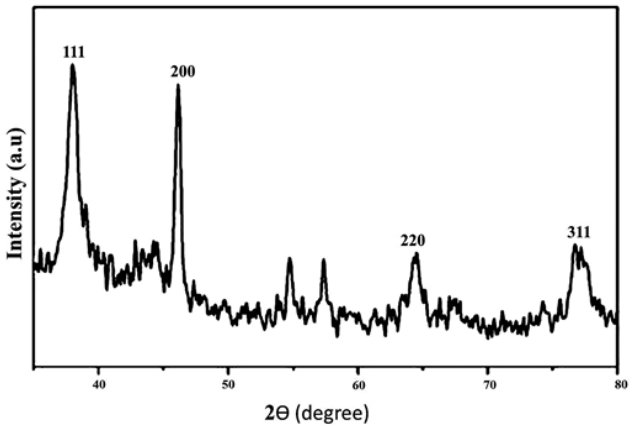

Fig. 5: X-ray diffraction patterns of the synthesized Ag NPs**.**

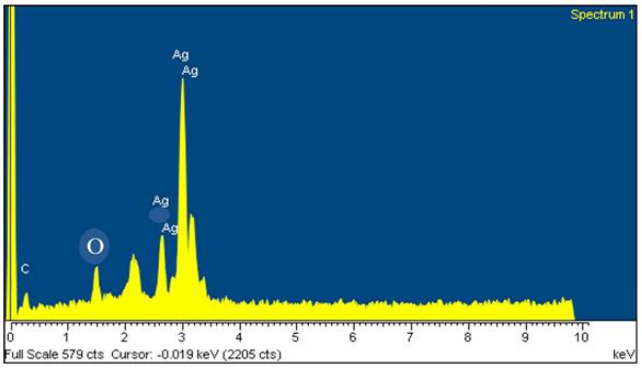

Fig. 6: EDX spectroscopy displays the purity and chemical composition of the biosynthesized Ag NPs.

Others suggested that, silver nanoparticles may disrupt transport systems, including ion efflux. The dysfunction of ion efflux can cause rapid accumulation of silver ions, which interrupts cellular processes such as metabolism and respiration by reacting with molecules. Stoimenov et al. [47] and Sondi and Salopek-Sondi [48] have depicted a new finding that the membrane could be deteriorated by the formation of pits and cavities on the surface cell wall membrane of the microorganism. This will increase the cell wall membrane permeability and directly irregular transport of cell fluids will occurred that result in the cell death. From the mentioned above, it is evident that the green-synthesized AgNPs is a good unique route, which is easily produced and can extensively has a great potential for use in controlling spore-producing fungal plant pathogens.

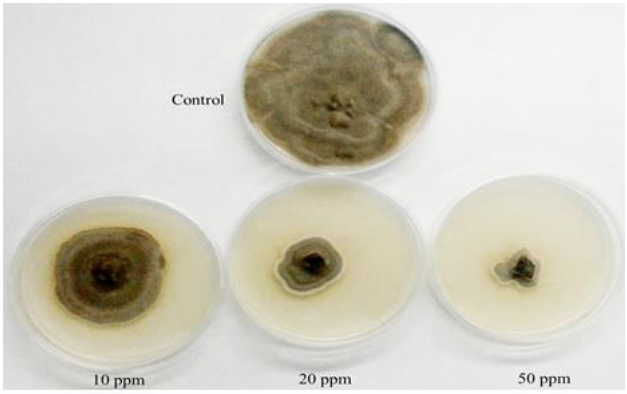

Fig. 1A

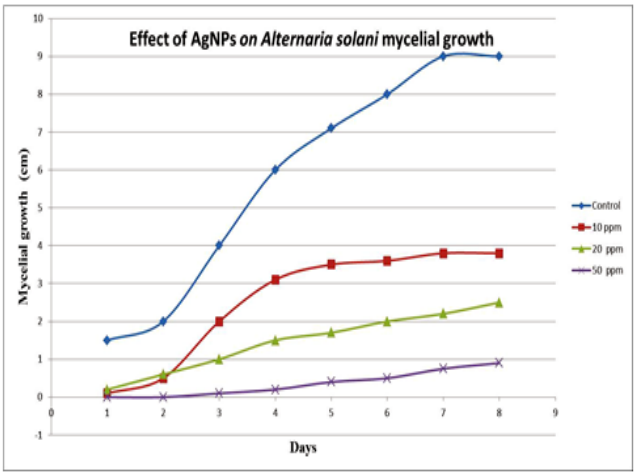

Fig. 7B

Fig. 7A: The inhibitory antifungal effect of biologically synthesized AgNPs of different concentrations (5, 10 and 20 ppm) against *Alternaria solani*. **Fig. 7B:** Effect of AgNPs on daily mycelial growth of *Alternaria solani*

4 Conclusion

In the present study, we have reported for the first time a one step, low cost and eco-friendly green approach for biosynthesis of AgNPs using aqueous solution of orsellinic acid without the addition of any external reducing/stabilizing agents. This single step procedure is highly suitable for large scale production as it is very fast and eliminates the elaborate processes employed in other bio-based protocols. The formed AgNPs were found to be highly stable, crystalline in nature and spherical in shape with an average diameter of 22.5 ±1.8 nm. The elemental composition confirmed the significant presence of Ag without other contaminants. Interestingly, AgNPs exhibited potent antifungal activity at comparatively low concentration against the phytopathogenic fungus *Alternaria solani* the causal agent of tomato early blight disease. Based on the present findings, we can conclude that the formed AgNPs could be exploited as potent antifungal agent in controlling various plant diseases caused by fungi. Although hydroxyl groups of orsellinic acid compound are suggested to involve in reduction of Ag+ ions and capping of the formed AgNPs, However, it necessitates further study to understand the exact mechanism by which silver nanoparticles enter into the fungal cell wall. Hence, more studies should be made using isolated pure compounds and their chemical structures should also be elucidated to unravel the puzzles of mycosynthesis mechanism.

Acknowledgment

A financial support from European Commission by Erasmus Mundus Scholarship-ACTION 2 WELCOME programme is gratefully acknowledged

References

[1] H. Karimi-Maleh, P. Biparva, M. Hatami, Biosens. *Bioelectron*. **48**, 270–275, (2013).

[2] R. Moradi, S.A. Sebt, H. Karimi-Maleh, R. Sadeghi, F. Karimi, A. Bahari, H. Arabi, Phy. Chem. *Chem. Phys*. **15**, 5888–5897, (2013).

[3] R. Sadeghi, H. Karimi-Maleh, M.A. Khalilzadeh, H. Beitollahi, Z. Ranjbarha, M.B. Pasha Zanousi, Environ. *Sci. Pollut. Res*. **20**, 6584–6593, (2013).

[4] M. Elyasi, M.A. Khalilzadeh, H. Karimi-Maleh, *Food Chem*. **141**, 4311–4317, (2013).

[5] A.A. Ensafi, H. Karimi-Maleh, *J. Electroanal. Chem*. **640**, 75–83, (2010).

[6] K. Natarajan, S. Selvaraj, M. V. Ramachandra. *Digest Journal of Nanomaterials and Biostructures*, **5**, 135-140, (2010).

[7] M. R. Bindhu, M. Umadevi. *Spectrochimica Acta Part A-Molecular and Bimolecular Spectroscopy*, **101**, 184-190, (2013).

[8] S.H. Jeong, S.Y. Yi, S.C. Yi. *Journals of Materials Science*, **40**, 5407-5411, (2005).

[9] X. Cao, C. Cheng, Y. Ma,C. Zhao. *Journal of Materials Science: Materials in Medicine*, **21**(10), 2861-2868, (2010).

[10] C.Y. Flores, A.G. Miñán, C.A. Grillo,R.C. Salvarezza, C. Vericat, P.L. Schilardi. *ACS Applied Materials & Interfaces*, **5**(8), 3149-3159, (2013).

[11] K.C. Pingali, D.A. Rockstraw, S. Deng. *Aerosol Science and Technology*, **39**(10), 1010-1014, (2005).

[12] X. Wang, J. Zuo, P. Keil. Grundmeier. *Nanotechnology*, **18**(26), 265-303, (2007).

[13] H.S. Shin, H.J. Yang, S.B. Kim, M.S. Lee. *Journal of Colloid and Interface Science*, **274**(1), 89-94, (2004).

[14] P. Mohanpuria, N. K. Rana, S. K. Yadav. *Journal of Nanoparticle Research*, 10, 507-517, (2008).

[15] T. Wang, L. Yang, B. Zhang, J. Liu. *Colloids and Surfaces B: Biointerfaces* **80**(1): 94–102, (2010).

[16] A. Prakash, S. Sharma, N. Ahmad, A. Ghosh, P. Sinha. *Journal of Biomaterials and Nanobiotechnology* **2**: 156–162, (2011).

[17] N. Jain, A. Bhargava, S. Majumdar, J.C. Tarafdar. *J. Nanoscale* **3**: 635–641 (2011).

[18] Apte, M., Girme, G., Bankar, A., Kumar, A.R., Zinjarde, S. *Journal of Nanobiotechnology* **11**: 2, (2013).

[19] Narayanan, K.B., Sakthivel, N. *Advances in colloid and Interface Science* **156**(1): 1–13, (2010).

[20] Birla, S., Tiwari, V., Gade, A., Ingle, A., Yadav, A., Rai, M. *Letters in Applied Microbiology* 48(2): 173–179. Blakemore, R. 1975. Magnetotactic bacteria. *Science* **190**(4212): 377–379, (2009).

[21] Strobel G, Daisy B, Castillo U, Harper J. Natural products from endophytic microorganisms. Journal of Natural Products. 2004; **67**: 257-268.

[22] AA. Gunatilaka. *Journal of Natural Product.* **69**: 505-526, (2006).

[23] V.C. Verma, R.N Kharmar, G.A Strobel. Natural Product Communications **4**: 1511-1532, (2009).

[24] C. Dipankar, S. Murugan. *Colloids and Surfaces B: Biointerfaces*, **98**, 112-119, (2012).

[25]V. C. Verma, R. N. Kharwar, A. C. Gange. *Nanomedicine*, **5**(1), 33-40, (2010).

[26] L. Liu, J. Yang, J. Xie, Z. Luo, J. Jiang, Y.Y. Yang, S. Liu. *Nanoscale*, **5**(9), 3834-3840, (2013).

[27] S. Tanvir, F. Oudet, S. Pulvin, W.A. Anderson. *Enzyme and Microbial Technology*, **51**(4), 231-236, (2012).

[28] V. Saharan, A. Mehrotra, R. Khatik, P. Rawal, S.S. Sharma, A. Pal, *Int. J. Biol. Macromol*. **62**, 677–683, (2013).

[29] X. Wang, Y. Du, H. Liu, *Carbohydr. Polym*. **56**, 21–26, (2004).

[30] W.L. Du, S.S. Niu, Y.L.Xu, Z.R.Xu, C.L. Fan, Carbohydr. Polym. **75**, 385–389, (2009).

[31] E. Corradini, M.R. de Moura, L.H.C. Mattoso, *Express Polym. Lett*. **4** (8), 509–515, (2010).

[32] M. Jaiswal, D. Chauhan, N. Sankararamakrishnan, *Environ. Sci. Pollut. Res.* **19**, 2055–2062, (2012).

[33] F. Brunel, N.E.E. Gueddari, B.M. Moerschbacher, *Carbohydr. Polym*. **92**, 1348–1356, (2013).

[34] J.B. Sinclair, O.D Dhingra. *Basic Plant Pathology Methods*. CRC Press, Boca Raton, Florida, USA, (1995).

[35]K.K.H. Domsch, W. Gams, T. H. Anderson. *Compendium of Soil Fungi*. Academic Press, London (1980).

[36] B. Ellis. *Dematiaceous Hyphomycetes*. CMI, Kew, Surrey, England, (1971).

[37] M. Gardes, T.D. Bruns. *Molecular Ecology*, **2**(2), 113-118, (1993).

[38] J. Smedsgaard. *J. Chromatogr*. A 760, 264–270, (1997).

[39]Y.H. Siddique, A. Fatima, S. Jyoti, F. Naz, W. Khan, B.R. Singh, A.H. Naqvi. *PloS one*, **8**(12), 80944, (2013).

[40] S. W. Kim, J. H. Jung, K. Lamsal, Y. S. Kim, J. S. Min, and Y. S. Lee .*Mycobiology*, vol. **40**, no. 1, pp. 53–58, (2012).

[41] Smedsgaard, J. *J. Chromatogr*.760, 264–270, (1997).

[42] S. W. Kim, J. H. Jung, K. Lamsal, Y. S. Kim, J. S. Min, and Y. S. Lee. *Mycobiology*, vol. **40**, no. 1, pp. 53–58, (2012).

[43] G. E. Evans, J. Staunton. *J. Chem. Soc. Perkin Trans.* **I**, 755-761, (1988).

[44] B. Baruwati, V. Polshettiwar, R.S. Varma. *Green Chemistry*, **11**(7), 926-930, (2009).

[45] S. Azizi, F. Namvar, M. Mahdavi, M.B. Ahmad, R. Mohamad. *Materials* **6**:5942–5950, (2013).

[46] M. Dubey, S. Bhadauria, B.S. Kushwah. *Journal of Nanomaterials and Biostructures*. **4**(3):537-543, (2009).

[47] P. K. Stoimenov, R. L. Klinger, G. L. Marchin, K. J. Klabunde, *Langmuir*, vol. **18**, no. 17, pp. 6679–6686, (2002).

[48] I. Sondi, B. Salopek-Sondi, *Journal of Colloid and Interface Science*, vol. **275**, no. 1, pp. 177–182, (2004).

[49] S. W. Kim, K. S. Kim, K. Lamsal et al., *Journal of Microbiology and Biotechnology*, vol. **19**, no. 8, pp. 760–764, (2009).

[50] M. Danilczuk, A. Lund, J. Sadlo, H. Yamada,J. Michalik, *Spectrochimica Acta—Part A:Molecular and Biomolecular Spectroscopy*, vol. **63**, no. 1, pp. 189–191, (2006).